JOURNAL OF SOLID STATE CHEMISTRY 82, 78–86 (1989)

X-Ray Absorption Study of the Ge–Se System

II. $GeSe_y$ Glasses: Bulk and Thin Film Samples

C. PEYROUTOU, S. PEYTAVIN, AND M. RIBES

Laboratoire de Physicochimie des Matériaux, USTL, 34060 Montpellier Cedex, France

AND H. DEXPERT

LURE, Bât. 209D, Université Paris-Sud, 91405 Orsay Cedex, France

Received February 21, 1989; in revised form May 1, 1989

EXAFS measurements on Se/Ge ratios greater than 2 have been undertaken for different forms of the $GeSe_y$ family, bulk or thin films. Data analysis was made both at the Ge and Se K edges and special attention was first paid to the effect of the grain size on the absorption amplitude. The results of the various investigations led to the conclusions that if the germanium tetrahedral environment is constant, that of selenium varies strongly between (i) $GeSe_3$ and $GeSe_y$, $y > 3$, and (ii) bulk phases and thin films. A model taking into account these differences is discussed, explaining these changes by the existence of selenium clustering in the more enriched Se compositions.

Introduction

X-ray absorption spectroscopy is a means of investigation widely used to obtain structural information from glassy compounds and the chalcogenide family has been one of the first studied by this technique. The germanium–selenium system presents a great number of different phases and, in a first work (1), we considered the $GeSe_2$ composition. This phase is obtained in either the crystallized or the vitreous states and the sample preparation conditions to acquire good EXAFS reference signals from crystallized samples have been particularly underlined. The effects of different grindings were discussed in detail, the knowledge of which opens the possibility of extracting information on the second shell surrounding the germanium atoms. As a consequence, a model related to the degree of depolymerization between the $GeSe_4$ linkages has been put forward. The present study is an extension of this work and considers first the particular case of the $GeSe_3$ phases. The research is then extended to the other $GeSe_y$ compositions we prepared, compositions where y is successively equal to either 3, 4, 6.6, 8.2, and 9.7 for bulk specimens or 2, 3, 3.3, and 6.5 for thin films.

I. Samples Preparation, Data Collection, and Analysis

I.A. Bulk Materials

Syntheses are made within quartz tubes using pure germanium and selenium pow-

0022-4596/89 $3.00

ders from Aldrich (gold label quality). They are mixed in appropriate proportions and introduced in the previously outgassed quartz cell which is sealed under high vacuum (10^{-5} Torr).

Depending on the composition and according to the phase diagram (2), a progressive heating (6°C per hr) is applied up to a temperature of 50 to 100°C greater than that of liquidus. A mechanical agitation of the furnace for several hours gives a good homogeneity to the melted mixture. The thermal treatment sequence ends by rapid quenching, the speed of which is chosen from the curve defined by Azoulay (*3*). The quenching constraints are then relaxed during a few hours of annealing at a temperature less than that of the vitreous transition *Tg*, as determined by microcalorimetry.

The chemical compositions of the prepared materials, bulk or thin films, have been systematically analyzed by energy dispersive X-ray measurements using a scanning microprobe. Within the experimental inaccuracy, the initial ratios between Ge and Se have been found again in the final products.

I.B. Thin Films

The $GeSe_y$ glasses are obtained from a laboratory and plasma enhanced chemical vapor deposition set up (PECVD) (*4, 5*) which allows the simultaneous deposition of the desired compositions onto a great number of silicon wafers. The precursors we used are GeH_4 and H_2Se, and as the deposit is plasma assisted, it can be made between room temperature and that of the vitreous transition.

I.C. Data Collection and Analysis

In all our experiments with bulk samples, powder or glassy specimens are mounted onto a polyacetate support and exposed to the X-rays from the monochromator, the thickness they cross being of the order of a few micrometers.

For the $GeSe_2$ thin films, as this chemical ratio corresponds to a defined and stable compound (*2*), the layers are obtained through a classical evaporation procedure by heating the crushed powders from a tantalum holder.

The experimental conditions of X-ray absorption recordings and analysis are the same as those described in Part I of this research (*1*). The grinding and grain size effects observed for the Se/Ge = 2 ratio were also at the $GeSe_3$ composition, these considerations giving us the inaccuracy limits of our analytical procedure.

II. Glassy $GeSe_3$: Grain Size Effect on the Absorption Amplitude

To eliminate any spurious thickness effects on the X-ray absorption signals and to check the validity of our sample conditioning for these measurements, a preliminary set of investigations is thus undertaken using $GeSe_3$ as a test specimen. Amorphous pieces of that composition are consequently crushed at different sizes calibrated through appropriate sieves and five powders are separated. Their diameters ϕ are: 80 μm or more; $40 < \phi < 80$ μm; $20 < \phi < 40$ μm; $10 < \phi < 20$ μm; and, finally, less than 20 μm.

The EXAFS signals are measured for each category of samples and the interaction dependance frequently observed in the literature between absorption and thickness is particularly noted. Different expected effects are observed—inhomogeneity within the size distribution, inhomogeneity of the grain deposition on the polyacetate support, etc.—and the inadequate materials rejected. These series of evaluations lead us to define a correct crushing and sizing procedure which allows one to obtain specimens for which the atomic arrangement does not vary during the sample conditioning.

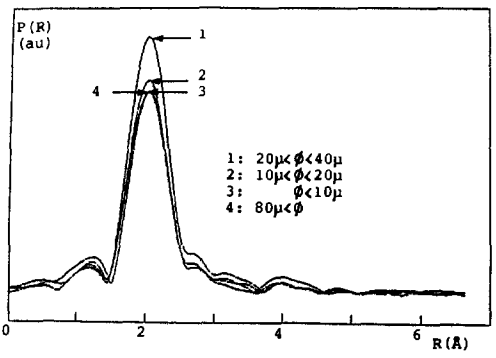

FIG. 1. Grain size effect at the germanium edge for the $GeSe_3$ glass (*FT* moduli uncorrected for phase shift).

II.A. Germanium Edge

With respect to the preceeding remarks, the Fourier transforms (*FT*) moduli reported in Fig. 1 are typical examples of the results we obtained. They give the error domain due to the amplitude dependance on the grain size and indicate the quality and reliability of our absorption measurements. For the first coordination sphere, uncorrected for phase shifts, the number of selenium neighbors N and the Ge–Se distance R vary very slightly around the mean values of 3.9 ± 0.2 for N and 2.36 ± 0.01 Å for R (Table I). Moreover, the adjustments we did on the second contribution, although this is of small intensity, show unambiguously that:

—the long Ge–Ge distances are very closely scattered around the mean value of 3.54 Å ± 0.02 Å;

—the second observable shell surrounding the germanium is slightly more stretched than the first one (± 0.25 around $N = 2.1$). The degree of depolymerization remains however quite unchanged whatever the strength of the grinding. The $GeSe_3$ amorphous phases are 33.6% depolymerized compared to the well-organized structure of the reference. We must recall here that D is the normalized difference between the average coordination number of germanium in the $GeSe_2$ network, 3.33, and its value N for the considered specimen:

$$D = \frac{3.33 - N}{3.33} \times 100.$$

II.B. Selenium Edge

Figure 2 shows the different *FT* moduli which present some disparities depending on the grain size, disparities however not in line with the linear evolution of the average

TABLE I

FIT RESULTS IN FUNCTION OF THE GRAIN SIZE AT THE GERMANIUM EDGE FOR THE FIRST AND SECOND COORDINATION SPHERES

$GeSe_3$ glass Grain size (μm)	First coordination sphere: Ge–Se bonds[a]					Second coordination sphere: long Ge–Ge distances[b]					
	N	R(Å)	$\Delta\sigma$(Å)	ΔE(eV)	$RF(10^{-4})$	N	R(Å)	$\Delta\sigma$(Å)	ΔE(eV)	$RF(10^{-3})$	D%
$\phi > 80$	3.90	2.36(5)	0.020	2.97	0.5	1.91	3.53(6)	0.020	2.97	0.9	42.5
$40 < \phi < 80$	4.00	2.36(4)	0.000	1.18	0.5	2.23	3.56(2)	0.020	2.96	0.9	33.0
$20 < \phi < 40$	3.70	2.36(3)	0.007	2.93	0.3	2.14	3.53(8)	0.020	2.75	1.3	35.6
$10 < \phi < 20$	4.00	2.36(4)	0.013	2.97	0.8	2.21	3.53(3)	0.020	2.97	1.7	33.6
$\phi < 10$	3.93	2.36(3)	0.016	2.97	0.5	2.18	3.54(4)	0.020	2.95	1.4	34.4

Note. *RF* and *D* are the reliability and depolymerization factors, respectively.

[a] Reference: $N = 4$, $R = 2.352$ Å.

[b] Reference: $N = 3.33$, $R = 3.599$ Å, $D = 0\%$.

TABLE II

FIT RESULTS IN FUNCTION OF THE GRAIN SIZE AT THE SELENIUM EDGE

$GeSe_3$ glass Grain size (μm)	First coordination sphere: Se–Se bonds[a]				
	N	R(Å)	$\Delta\sigma$(Å)	ΔE(eV)	$RF(10^{-5})$
$\phi > 80$	1.25	2.36(2)	0.000	0.00	0.7
$20 < \phi < 40$	1.60	2.36(0)	0.002	−0.48	0.8
$10 < \phi < 20$	1.33	2.36(1)	0.007	−0.06	0.2
$\phi < 10$	1.32	2.36(9)	0.020	0.95	0.8

[a] Reference: $N = 2$, $R = 2.352$ Å.

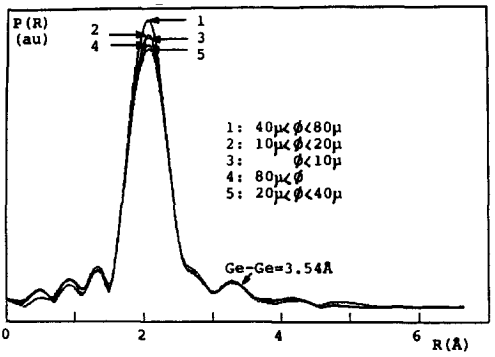

FIG. 2. Grain size effect at the selenium edge for the $GeSe_3$ glass (*FT* moduli uncorrected for phase shift).

diameter. This could be explained by the fact that, at the selenium edge, the signal is practically half that of germanium, so that change in the experimental amplitude introduces a larger fluctuation than for the case of germanium. We must nevertheless point out that the coordination numbers given by the fitting procedure are abnormally low ($1.33 < N < 1.60$) compared to the expected value, $N = 2$ (Table II). This result is hardly understandable without turning to a chemical substitution which could occur in the selenium environment. Such a hypothesis will be discussed later, after a full description of the other components of that system is presented. It is in any case important to keep in mind that for the germanium environment in $GeSe_3$ glasses the present grain size considerations lead to the general conclusion that:

—the tetrahedral $GeSe_4$ entity is preserved, and

—the degree of depolymerization D is kept constant whatever the nature of the crushing ($\overline{D} = 35.8\%$).

III. Bulk (y = 3, 4, 6.6, 8.2, 9.7) and Thin Films (y = 2, 3, 3.3, 6.5) of $GeSe_y$ Compositions

III.A. Germanium Edge

In any case, bulk samples or thin films, the germanium atom keeps a tetrahedral environment with practically the same Ge–Se distances: $R = 2.37 \pm 0.01$ Å (bulk) or 2.36 ± 0.01 Å (thin films) (Tables III and IV).

TABLE III

FIT RESULTS AT THE GERMANIUM EDGE FOR THE DIFFERENT VITREOUS BULK SAMPLES

	First coordination sphere: Ge–Se bonds[a]					Second coordination sphere: long Ge–Ge distances[b]					
	N	R(Å)	$\Delta\sigma$(Å)	ΔE(eV)	$RF(10^{-4})$	N	R(Å)	$\Delta\sigma$(Å)	ΔE(eV)	$RF(10^{-3})$	D%
$GeSe_3$	3.99	2.37(2)	0.020	2.86	1.5	2.24	3.55(7)	0.020	2.95	1.2	32.7
$GeSe_4$	3.99	2.36(9)	0.001	2.10	0.6	2.34	3.53(6)	0.018	2.97	6.9	29.7
$GeSe_{6.6}$	4.00	2.37(2)	0.000	2.27	0.7	2.82	3.54(9)	0.020	2.97	1.0	15.3
$GeSe_{8.2}$	4.00	2.37(4)	0.001	2.97	0.8	2.65	3.54(8)	0.020	2.96	0.9	20.4
$GeSe_{9.7}$	4.00	2.37(5)	0.000	2.97	0.9	2.52	3.55(4)	0.020	2.97	0.9	24.3

[a] Reference: $N = 4$, $R = 2.352$ Å.
[b] Reference: $N = 3.33$, $R = 3.599$ Å, $D = 0\%$.

TABLE IV

FIT RESULTS AT THE GERMANIUM EDGE FOR THE THIN FILMS

	First coordination sphere: Ge–Se bonds[a]					Second coordination sphere: long Ge–Ge distances[b]					
	N	R(Å)	$\Delta\sigma$(Å)	ΔE(eV)	$RF(10^{-4})$	N	R(Å)	$\Delta\sigma$(Å)	ΔE(eV)	$RF(10^{-2})$	D%
$GeSe_2$ (evaporation)	4.00	2.36(3)	0.010	2.72	0.9	1.81	3.55(1)	0.020	2.96	0.3	45.6
$GeSe_3$(PECVD)	4.00	2.36(4)	0.000	2.97	1.6	2.06	3.52(5)	0.020	2.95	0.3	38.0
$GeSe_{3.3}$(PECVD)	4.00	2.36(3)	0.001	2.97	7.5	2.05	3.52(1)	0.020	2.97	0.2	38.0
$GeSe_{6.5}$(PECVD)	4.00	2.37(3)	0.004	2.97	2.2	1.97	3.54(6)	0.020	2.97	0.1	40.8

[a] Reference: $N = 4$, $R = 2.352$ Å.
[b] Reference: $N = 3.33$, $R = 3.599$ Å, $D = 0\%$.

There is a slight trend for a bond length shortening of the bridged

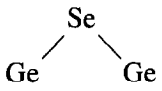

linkages between thin films (3.53 ± 0.02 Å) compared to bulk samples (3.55 ± 0.01 Å). The films are, as expected, more depolymerized than the bulk: the calculated value of D is 38.5% for PECVD specimens, 45.56% for the films prepared by evaporation, and 24.5% for the bulk samples.

In fact, the results obtained for the films are very close to those relative to the bulk amorphous $GeSe_2$ (*1*): in particular the D factors are quite similar (D (a-$GeSe_2$) = 45.7%).

TABLE V

FIT RESULTS AT THE SELENIUM EDGE FOR THE BULK SAMPLES AND THE THIN FILMS

	First coordination sphere: Se–Se bonds[a]				
Bulk samples	N	R(Å)	$\Delta\sigma$(Å)	ΔE(eV)	$RF(10^{-4})$
$GeSe_3$	1.40	2.36(0)	0.006	1.28	0.5
$GeSe_4$	1.68	2.36(1)	0.000	1.25	0.4
$GeSe_{6.6}$	1.46	2.35(9)	0.000	0.75	0.3
$GeSe_{8.2}$	1.63	2.36(0)	0.003	0.94	0.4
$GeSe_{9.7}$	1.53	2.35(9)	0.005	0.95	0.7
Thin films					
$GeSe_2$ (evaporation)	1.98	2.35(6)	0.018	0.65	0.1
$GeSe_3$ (PECVD)	1.87	2.35(6)	0.000	−0.88	0.1
$GeSe_{3.3}$ (PECVD)	1.90	2.35(9)	0.001	−0.34	0.1
$GeSe_{6.5}$ (PECVD)	1.76	2.36(2)	0.000	−0.84	0.3

[a] Reference: $N = 2$, $R = 2.352$ Å.

III.B. Selenium Edge

The abnormal difference already mentioned during the granolometric study of the $GeSe_3$ glasses—that is, a coordination number largely inferior to 2—is still found for the selenium-enriched glasses: an average of 1.54 ± 0.15 neighbor is calculated (Table V). On the contrary, for the thin films, this mean number, 1.87 ± 0.11, is closer to the normal value. The distances we determined in both cases are identical: $R = 2.35(8)$ Å for the films and 2.35(9) Å for the bulk species.

To strengthen the reliability of these simulations, we have reported in Fig. 3 the plot of ln ($\chi(k)$ amorphous/$\chi(k)$ crystal) as a function of the photoelectron wavevector

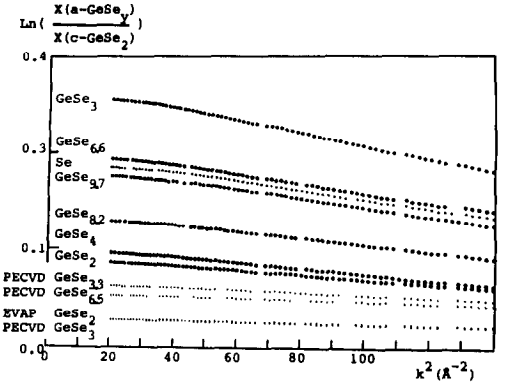

FIG. 3. Plot of the ln ($\chi(k)$ glass/$\chi(k)$ crystal) = $f(k^2)$ curves at the selenium edge for the bulk samples and the thin films.

TABLE VI

MEASURED VALUES OF THE NEIGHBORS NUMBER (N) AND THE DEBYE–WALLER FACTOR ($\Delta\sigma$) AT THE SELENIUM EDGE FOR VARIOUS GLASS AND CRYSTALLIZED PHASES (BULK OR THIN FILMS)

Bulk samples	N	$\Delta\sigma^2$ (10^{-4} Å^2)
$GeSe_2$ vitreous	1.82	1.1
$GeSe_3$ vitreous	1.52	3.3
$GeSe_4$ vitreous	1.80	1.4
$GeSe_{6.6}$ vitreous	1.62	2.4
$GeSe_{8.2}$ vitreous	1.74	1.7
$GeSe_{9.7}$ vitreous	1.65	2.5
Se	1.63	2.5
Thin films		
$GeSe_2$ (evaporation)	1.94	0.3
$GeSe_3$ (PECVD)	1.94	0.3
$GeSe_{3.3}$ (PECVD)	1.87	0.7
$GeSe_{6.5}$ (PECVD)	1.89	0.4

k^2, where χ is the EXAFS experimental absorption signal. This ratio allows us to decorrelate the number of neighbors from the Debye-Waller factor $\Delta\sigma$ and is consequently very useful as the decrease of the amplitude may either come from a loss of neighbors or from an increase in the static disorder. The crystallized reference we took is c-$GeSe_2$ and all the other samples are therefore compared to it. For completeness, the curve of pure selenium is also given. Although the environment is not of the same nature, it constitutes nevertheless the limit for the selenium-enriched phases. This is reasonable as Ge and Se are not far away from each other in the periodic table, so that their X-ray cross sections are almost the same. The values of N and $\Delta\sigma^2$ measured from that figure are listed in Table VI. They fully confirm the results listed in Tables II and V and give a greater credibility to our fitting procedure.

One could however be surprised by the low value found for the selenium neighbor number in pure selenium, 1.63, instead of 2 as it is usually accepted. Let us note here that this number comes from an analysis which fits the experimental selenium signal with backscattered phase and amplitude extracted from c-$GeSe_2$. As we pointed out above, although the germanium X-ray cross section is slightly weaker than that of selenium, this is not enough to explain the significant decrease in amplitude. The main cause is due to the selenium sample itself, as it is well known from the literature (*6*) that this element exists under various polymorphs which present Se–Se distances in between 2.33 to 2.37 Å. The common form is amorphous and the ordered networks are either helicoidal or cyclic, all these varieties being more or less difficult to isolate from each other. These considerations lead us to prefer the selenium backscattering parameters from the c-$GeSe_2$ phase as this material is more regular.

IV. Discussion of the EXAFS Analysis

As the germanium environment remains quite unchanged over the whole range of compositions and morphologies we investigated, the essential part of the discussion will deal with the selenium environment, key to our model. Figure 3 and Table V illustrate the comparisons which support the different arguments.

For the bulk samples, since the selenium concentration is enhanced within the glass from the $GeSe_2$ composition, we observed a trend to decrease the selenium coordinence down to the value we calculated for the pure element, 1.63. The triselenide, $GeSe_3$, seems to loose an even greater number of neighbors as the small value we found, 1.4, cannot be due totally to an eventual increase in the Debye–Waller factor: this parameter, as in the other compositions, keeps in fact the same low value, always less than 0.01 Å. The idea which thus comes directly to mind to explain this general decrease is that if the selenium atom is linked to germanium, it must be also in sight with other seleniums. Their number

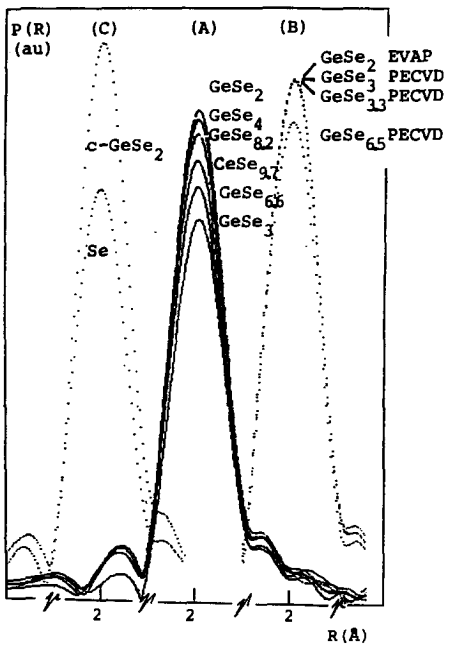

FIG. 4. Selenium edge: Comparison of the *FT* moduli obtained from bulk samples (A), thin films (B), and references compounds (C). The signals are uncorrected for phase shift, (B) and (C) being displaced by ±1 Å on each side of (A).

could also depend then on the degree of completion the reaction has locally reached, some of the selenium not entering in the formation of the $GeSe_4$ polyhedron.

The situation looks different for thin films: the logarithmic plot of Fig. 3 shows clearly not only that the selenium coordinence is close to that of bulk $GeSe_2$, but also that the Debye–Waller factors of all these films are practically the same as for the bulk phase. Figure 4 compares all these different *FT* moduli. To be as clear as possible, the dotted curves relative to the reference compounds (*c*-$GeSe_2$ and pure Se) on the one hand, and to thin films on the other, have arbitrarily shifted by one angstrom from their position in the bulk samples.

If one attempts to explain the low selenium coordinance of the bulk phases, three hypotheses must be ruled out before discussing the above experimental curves and simulations:

—the study made on the grain size effect on the absorption intensity of $GeSe_3$ demonstrates that the differences in amplitude are not coming from that point;

—a real lowering of the coordination number is not likely since: (i) interatomic distances do not change significantly and (ii) the germanium neighboring remains constant;

—the number of dangling bonds is probably not very high unless it will be in contradiction with the fact that the *FT* moduli of the bulk glasses are not too different from those of amorphous $GeSe_2$ and thin films.

The explanation we propose is thus the existence of two neighborhood components for selenium. They are composed of germanium from the $GeSe_4$ polyhedra and of some atoms of selenium which do not belong to this network, linking these polyhedra, the proportion of which depends on the starting composition of the mixture and on the reacting conditions. This phenomenon is in fact the first step of the segregation process which leads to the formation of Se clusters for higher Se/Ge ratios. Great differences seem to exist between these components:

(i) $GeSe_3$ and the $GeSe_y$ with $y > 3$ bulk phases;

(ii) bulk phases and thin films.

These segregated atoms of selenium form likely chains or microdomains in which the Se–Se distances are not very regular, a situation which could be similar to that existing for the pure selenium we used for comparison. We must point out here that this conclusion is in line with the electron microscopy study made by Yi *et al.* who image Se clustering for the same compositions (*7*). We must recall here that we have been unable to appreciate this scattering of distances when fitting the standard selenium

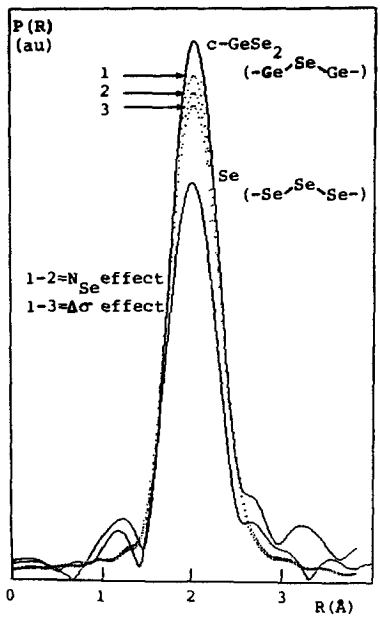

FIG. 5. Simulations of the chemical substitution and static disorder effects on the neighboring of a selenium atom. The calculated *FT* moduli (1), (2), and (3) are compared to the experimental signals measured on *c*-$GeSe_2$ and pure selenium. The different combinations which have been considered are: (1) 0.1 Se + 1.9 Ge, $\Delta\sigma$ (Se or Ge) = 0.0 Å; (2) 0.3 Se + 1.7 Ge, $\Delta\sigma$ (Se or Ge) = 0.0 Å; (3) 0.1 Se + 1.9 Ge, $\Delta\sigma$ (Se or Ge) = 0.02 Å.

with the amplitude and phase shift extracted from *c*-$GeSe_2$. It is thus obvious that the refinements of these $GeSe_y$ phases are very limited in their conclusion at the selenium edge.

We have however tried to estimate what could be the validity of this hypothesis of a mixed (Ge + Se) surrounding, taking the backscattering parameters from the pure selenium and not from the crystallized diselenide. The *FT* modulus of selenium is then considered to come from two neighbors at an average of 2.352 Å (these values are 1.63 and 2.360 Å when using $GeSe_2$ as reference). Three calculations have been made and Fig. 5 reports the corresponding plots:

—first simulation: 0.1 Se + 1.9 Ge, $\Delta\sigma$ (Se or Ge) = 0 Å;

—second simulation: 0.3 Se + 1.7 Ge, $\Delta\sigma$ (Se or Ge) = 0 Å;

—third simulation: 0.1 Se + 1.9 Ge, $\Delta\sigma$ (Se or Ge) = 0.2 Å.

It is clear from Fig. 5 that introducing small fractions of selenium (5 or 15% for simulation 1 or 2) decreases significantly the overall amplitude, a phenomenon which is, as expected, accentuated when adding static disorder (third simulation). Besides these points, the fits show the extreme difficulty of separating the two effects, chemical substitution and/or distance scattering, as an equivalent decrease is obtained in changing the Debye–Waller difference by 0.02 Å.

Conclusion

The loss of amplitude registered at the selenium edge of the bulk vitreous phases is thus related to the existence of Se–Se pairs, the lengths of which are probably scattered over several hundreds of angstroms. Differences exist in function of the Se/Ge ratios, likely in connection with a percolation/demixion phenomenon as described in Refs. *8* to *12*. As a matter of fact, if we suppose:

(i) that the predominant situation is the outrigger raft at the $GeSe_2$ composition;

(ii) that the incoming selenium atoms integer this raft, leading to a more rigid vitreous network from $GeSe_2$ to $GeSe_3$, it is certain that such behavior will increase the stretch in distances.

If the same model is applied further on, for the phases after the $GeSe_4$ composition, the rigid zones of the glass percolate correspond to demixing chains of the selenium. By the way, the glass is less and less overconstraint as for $GeSe_3$, and the dispersion of distances becomes smaller. The loss in

FT amplitude is here more and more due to a higher number of selenium pairs; the germanium environment which could have been slightly distorted within the overconstraint glass, relaxes and becomes more regular. This point is in line with the fact that at the Ge absorption edge, the depolymerization which goes down to $GeSe_4$ remains constant for higher Se/Ge ratios.

These conclusions are not valid for thin films where the mixed selenium environment has not been detected, even for greatly enriched selenium compositions. Other preparations of $GeSe_3$ or $GeSe_5$ obtained respectively by evaporation and PECVD present the same behavior. No satisfactory explanation or model can be advanced at the present time. More work is thus planned and if the X-ray absorption measurements presented here will have been made in the transmission mode, we expect to realize in the near future surface experiments using an electron detection system (*13*) which will give us the possibility of drawing depth profiles from a few nanometers to one micrometer.

References

1. C. PEYROUTOU, S. PEYTAVIN, M. RIBES, AND H. DEXPERT, *J. Solid State Chem.* **81,** 70 (1989).
2. L. BALDE, Thèse Doctorat d'Etat Paris VI (1981).
3. R. AZOULAY, H. THIBIERGE, AND A. BRENAC, *J. Non-Cryst. Solids* **18,** 33 (1975).
4. M. RIBES, M. MAURIN, B. CROS, S. PEYTAVIN, P. JULIEN, AND F. XINXO, *Brev. Français* 36/03.395 Extension Europe/U.S.A./Japan FR/87/00057.
5. M. RIBES, B. CROS, AND P. JULIEN, "SPIE Proc., Optical Microlithography," Vol. 811, 202, The Hague (1987).
6. A. F. WELLS, "Structural Inorganic Chemistry," Oxford Univ. Press (Clarendon), London/New York (1984).
7. J. J. L. YI AND P. R. STRUTT, *J. Non-Cryst. Solids* **102,** 228 (1988).
8. S. ASOKAN, G. PARTHASARATHY, AND E. S. R. GOPAL, *Phys. Rev. B* **35,** 8269 (1987).
9. M. F. THORPE, *J. Non-Cryst. Solids* **57,** 355 (1983).
10. J. C. PHILLIPS, *J. Non-Cryst. Solids* **34,** 153 (1979) and **43,** 37 (1981).
11. J. C. PHILLIPS, *Phys. Rev. B* **31,** 8157 (1985).
12. J. C. PHILLIPPS, *in* "Proceedings of the Symposium on Inorganic Resist Systems" D. A. Doane, and A. Heller, Eds.), Vol. 82–9, p. 147 (1982).
13. G. TOURILLON, E. DARTYGE, A. FONTAINE, M. LEMONNIER, AND F. BARTOL *Phys. Lett. A* **121,** 251 (1987).